

A Beam of Metastable Krypton Atoms Extracted from an RF-Driven Discharge

C.Y. Chen,^a K. Bailey,^a X. Du,^{a,c} Y.M. Li,^a Z.-T. Lu,^{a*} T.P. O'Connor,^a L. Young,^b G. Winkler^d

^aPhysics Division, ^bChemistry Division, Argonne National Laboratory, Argonne, Illinois 60439

^cPhysics and Astronomy Department, Northwestern University, Evanston, Illinois 60208

^dInstitute for Isotope Research and Nuclear Physics, University of Vienna, Vienna, Austria

An RF-driven discharge is used to produce a beam of metastable krypton atoms at the $5s[3/2]_2$ level with the angular flux density of $4 \times 10^{14} \text{ s}^{-1} \text{sr}^{-1}$ and the most-probable velocity of 290 m/s, while consuming 7×10^{16} krypton atoms/s. When operated in a gas-recirculation mode, the source consumes 2×10^{15} krypton atoms/s with the same atomic-beam output.

* Email: lu@anl.gov

Thermal beams of metastable noble gas atoms have a wide range of applications including atom lithography,¹ atom holography,² atom optics,³ atomic collision studies,⁴ and precision measurements.⁵ Sources of such beams have been developed based on electron-impact excitation where energetic electrons are produced in various ways such as an electron beam,⁶ a DC glow discharge,⁷ or a surface-wave-sustained plasma.⁸ These sources produce intense metastable atomic beams with angular flux densities in the range of 10^{13} - 10^{15} s⁻¹sr⁻¹. The gas consumption rate, however, has not been a primary design concern, and has so far been neglected in publications. This is because the aforementioned applications use gases that are readily available in large quantities (> 1000 cm³ STP). The recent demonstration of Atom Trap Trace Analysis,⁹ in which laser manipulation of metastable krypton (Kr*) atoms was used to count atoms of rare krypton isotopes, has motivated our development of an efficient source of Kr* atoms that can accommodate a small amount of gas (~ 1 cm³ STP).

In this source Kr atoms are excited to the $5s[3/2]_2$ metastable level (lifetime ≈ 40 s) in an RF-driven discharge. As schematically shown in Figure 1, Kr gas flows through a discharge region that fills the inside of a quartz-glass tube. The pressure in the source chamber is 3 mTorr and the pressure in the intermediate chamber is about 10^{-5} Torr. The discharge is driven by a coaxial RF resonator that consists of a copper coil enclosed in a brass shield (Fig. 2).¹⁰ The resonator resonates at 155 MHz with an un-loaded Q of 38, and typically receives 7 Watts of RF power.

We determine the flux and the velocity distribution using laser spectroscopy techniques with a diode laser whose wavelength is tuned to the resonance of the $5s[3/2]_2$ - $5p[5/2]_3$ transition at 811 nm. Two laser beams intersect with the atomic beam at a distance of 66 cm downstream from

the exit of the discharge tube (Fig. 1). Figure 3 shows the atomic fluorescence signal detected by a photodiode detector as the laser frequency is scanned through the resonance. One of the laser beams, directed perpendicular to the atomic beam, provides the zero-Doppler-shifted fluorescence signal that appears as narrow peaks. Based on this signal, we calculate that 4×10^5 $^{84}\text{Kr}^*$ (isotopic abundance = 57%) atoms are present in the fluorescing volume of 0.2 cm^3 . The other laser beam, directed at an angle of 45° to the atomic beam, provides the Doppler-shifted fluorescence that appears as a broad peak. Based on this signal, we calculate that the most probable velocity is 290 m/s. The density of Kr^* atoms in the fluorescing region ($4 \times 10^6 \text{ cm}^{-3}$), multiplied by the most probable velocity, gives the flux density of $1 \times 10^{11} \text{ s}^{-1} \text{ cm}^{-2}$. Given that the fluorescing region is 66 cm from the source exit, we conclude that the angular flux density of the Kr^* atomic beam is $4 \times 10^{14} \text{ s}^{-1} \text{ sr}^{-1}$. We attempted to increase the flux by doubling the RF power and by adding a longitudinal magnetic field. In each case, a brighter discharge was visually observed but the flux was increased by less than 20%. It seems that the operating condition is near the equilibrium between the excitation and the ionization processes.

Higher source efficiencies are achieved with gas recirculation.¹¹ Depending on valve settings, the gas in the intermediate chamber can either be pumped out (Fig. 1), or be redirected back to the source chamber, via a 150 liters/s turbo pump. The conductance between the source chamber and the intermediate chamber is limited, by a collimator, to 1.3 liters/s. The recirculated gas is purified with a LN_2 -cooled trap. We measure that the source consumes $7 \times 10^{16} \text{ Kr atoms/s}$ ($3 \times 10^3 \text{ cm}^3 \text{ STP/s}$) without recirculation, and $2 \times 10^{15} \text{ Kr atoms/s}$ ($1 \times 10^4 \text{ cm}^3 \text{ STP/s}$) with recirculation. Therefore, the recirculation helps improve the source efficiency by a factor of 35. Further improvement is possible by optimizing the geometry of the collimator between the two

chambers. The flux density of Kr (ground-level) atoms in the forward direction is roughly measured by noting the change of vacuum pressure in the analysis chamber. We estimate that the ratio of Kr* flux over Kr flux is approximately 10^{-3} in the forward direction.

This source is easy to operate and maintain. The discharge can be started at the operating gas flow condition by raising the RF power to 14 W for a few seconds. Once ignited, the discharge and the metastable beam flux are stable. Moreover, this source uses no electrodes and needs less maintenance effort compared with other types of discharge sources that often require regular changes of electrodes due to sputtering problems.

We thank R. Pardo for the suggestion of using an RF-driven discharge. We thank K.W. Shepard, B. Lehmann, and G. Sprouse for helpful discussions. This work is supported by the U.S. Department of Energy, Nuclear Physics Division, and LY by the Office of Basic Energy Sciences, Division of Chemical Sciences, under contract W-31-109-ENG-38.

1. K.K. Berggren, A. Bard, J.L. Wibur, J.D. Gillaspay, A.G. Helg, J.J. McClelland, S.L. Rolston, W.D. Phillips, M. Prentiss, G.M. Whitesides. *Science* **269**, 1255 (1995).
2. M. Morinaga, M. Yasuda, T. Kishimoto, F. Shimizu. *Phys. Rev. Lett.* **77**, 802 (1996).
3. D.M. Giltner, R.W. McGowan, S.A. Lee. *Phys. Rev. Lett.* **75**, 2638 (1995).
4. M. Walhout, U. Sterr, C. Orzel, M. Hoogerland, S.L. Rolston, *Phys. Rev. Lett.* **74**, 506 (1995).
5. F. Minardi, G. Bianchini, P.C. Pastor, G. Giusfredi, F.S. Pavone, M. Inguscio, *Phys. Rev. Lett.* **82**, 1112 (1999).

6. R.S. Freund, Rev. Sci. Instr. **41**, 1213 (1970). R.D. Rundel, F.B. Dunning, R.F. Stebbings, Rev. Sci. Instr. **45**, 116 (1974). B. Brutschy and H. Haberland, J. Phys. **E10**, 90 (1977). T.W. Riddle, M. Onellion, F.B. Dunning, G.K. Walters, Rev. Sci. Instr. **52**, 797 (1981).
7. D.W. Fahey, W.F. Parks, L.D. Schearer, J. Phys. **E13**, 381 (1980). M.J. Verheijen, H.C. Beijerinck, L.H.A.M. v.Moll, J. Driessen, N.F. Verster, J. Phys. **E17**, 904 (1984). J.A. Brand, J.E. Furst, T.J. Gay, L.D. Schearer, Rev. Sci. Instr. **63**, 163 (1992). J. Kawanaka, M. Hagiuda, K. Shimizu, F. Shimizu, H. Takuma, Appl. Phys. **B56**, 21 (1993). W. Rooijackers, W. Hogervorst, W. Vassen, Opt. Comm. **123**, 321 (1996).
8. M.E. Bannister and J.L. Cecchi, J. Vac. Sci. Technol. **A12** , 106 (1994).
9. C.Y. Chen, Y.M. Li, K. Bailey, T.P. O'Connor, L. Young, Z.-T. Lu, Science **286**, 1139 (1999).
10. W.W. Macalpine and R. O. Schildknecht, Proceedings of the IRE, 2099 (Dec. 1959).
11. B.E. Lehmann, D.F. Rauber, N. Thonnard, R.D. Willis, Nucl. Instr. Meth. **B28**, 571 (1987).

Fig. 1 A schematic of the experimental setup.

Fig. 2 A schematic of the RF resonator. (1) Copper wire; 11 turns, wire diameter = 1.5 mm. (2) Brass shield. (3) Quartz-glass tube; 1.0 cm inner diameter. (4) Ceramic spacer.

Fig. 3 Kr* beam fluorescence vs. laser frequency. The three zero-Doppler shifted peaks are due to three isotopes, $^{82}\text{Kr}^*$, $^{84}\text{Kr}^*$, and $^{86}\text{Kr}^*$, whose isotopic abundances are 11%, 57%, and 17%, respectively. At the low-velocity side, the measured velocity distribution deviates from the Maxwell-Boltzmann distribution, possibly due to a velocity-dependent quenching effect.

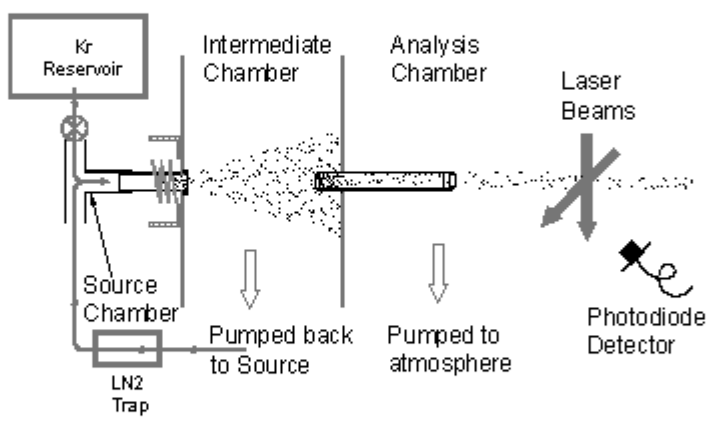


Figure 1

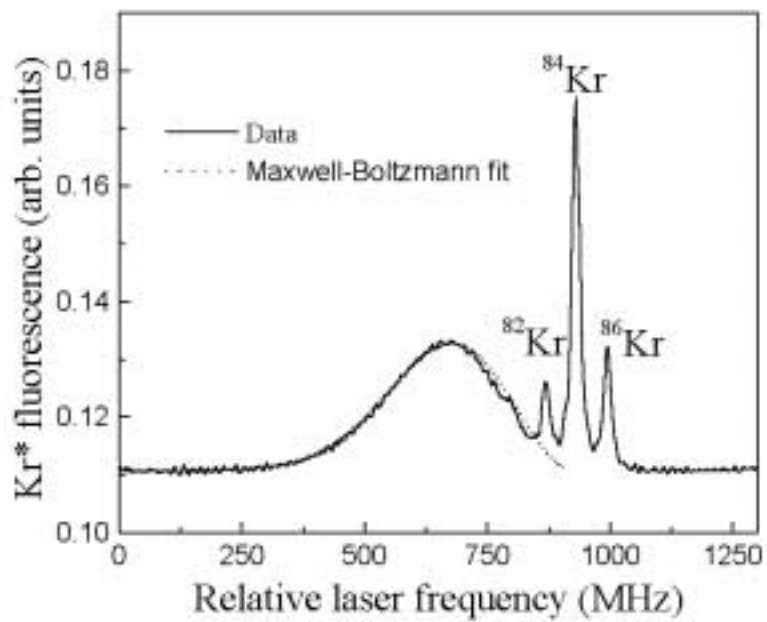


Figure 3

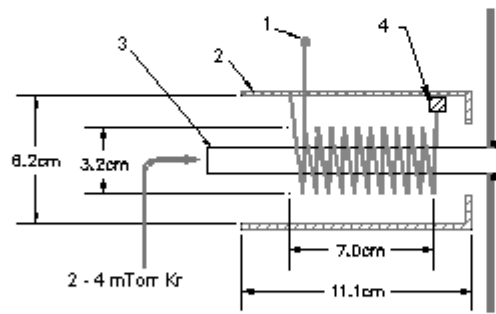


Figure 2